Matrix-Isolation FTIR Spectroscopic and DFT Studies of the XMNN (X=Cl, Br, M=Cu, Ni) Molecules

Mohua Chen, Mingfei Zhou,* Luning Zhang, and Qizong Qin

Laser Chemistry Institute, Fudan University, Shanghai 200433, P. R. China

Received: March 28, 2000; In Final Form: July 10, 2000

The ClCuNN, BrCuNN, and ClNiNN molecules have been prepared and isolated in solid argon by co-condensation of the species generated from 1064 nm laser ablation of copper or nickel halides with N_2/Ar gas mixtures. On the basis of isotopic substituted experiments and density functional theory calculations, infrared absorptions at 2296.3, 2297.8, and 2246.3 cm^{-1} are assigned to the N−N stretching vibrations of the linear molecules, ClCuNN, BrCuNN, and ClNiNN in solid argon, respectively. The binding energies for ClCuNN, BrCuNN, and ClNiNN with respect to MX (M=Cu, Ni, X=Cl, Br) and N_2 were computationally estimated to be 20.4, 18.7, and 18.9 kcal/mol, respectively.

Introduction

Coordination of dinitrogen with transition metal centers is the initial step of the complex sequential chemical activation of dinitrogen. A number of experimental and theoretical studies have been carried out to examine the interactions of transition metal atoms and cations with dinitrogen.[1−14] The dinitrogen complexes of transition metals have been identified using matrix isolation spectroscopy, and both end-bonded and side-bonded dinitrogen complexes were reported.[1−5] By using ion cyclotron resonance mass spectrometric and photodissociation excitation spectroscopic techniques, the interactions between transition metal cations and dinitrogen have also been studied in the gas phase. The bond energies of the transition metal cation−N_2 complexes such as Cr^+−N_2, Fe^+−N_2, Co^+−N_2, and Ni^+−N_2 have been measured.[6−11] The theoretical studies indicated that the ground-state geometries of metal cation-N_2 complexes have linear end-bonded symmetry, which is favored over the side-bonded arrangement due to the directional properties of the permanent quadrupole moment of N_2.[12−14] However, a side-bonded structure was proposed for the ground-state $Co^+(N_2)$ complex. [9]

Matrix isolation-infrared spectroscopy has proven to be a highly effective method for the characterization of transition metal compounds with weakly bound ligands.[15−17] Because of the perturbations caused by the coordinated metals, the N−N stretching vibration becomes observable in the infrared spectrum. Different coordination modes will result in the frequency shifts and the different structures in the isotope mixed experiment. In this paper, we report a combined matrix isolation FTIR spectroscopic and DFT study on the copper and nickel monohalides dinitrogen complexes generated from the reaction of laser ablated copper and nickel halides with N_2 molecules.

Experimental and Theoretical Methods

The technique used for pulsed laser ablation and matrix isolation infrared spectroscopic investigation has been described in detail previously.[18] The 1064 nm fundamental of a Nd:YAG laser (Spectra Physics, DCR 2, 20 Hz repetition rate and 8 ns pulsed width) was focused onto a rotating metal halide target through a hole in a CsI window. Typically, 5∼10 mJ/pulse laser power was used. The ablated metal halides were co-deposited with molecular N_2 in excess argon onto a 11 K CsI window at a rate of 2∼4 mmol/h. The CsI window was mounted on a copper holder at the cold end of the cryostat (Air Products Displex DE 202) and maintained by a closed-cycle helium refrigerator (Air Products Displex 1R02W). The FTIR spectra were recorded by a Bruker IFS 113v Fourier transform infrared spectrometer equipped with a DTGS detector with a resolution of 0.5 cm^{-1}. Dinitrogen (Shanghai BOC, 99.5%), isotopic $^{15}N_2$ (99%, Matheson), and $^{14}N_2$+$^{14}N^{15}N$+$^{15}N_2$ mixtures (45% + 10% + 45%) prepared by discharge of mixed $^{14}N_2$+$^{15}N_2$ (50% + 50%) were used in different experiments. The annealing experiments were done by warming up the sample deposit to the desired temperature and quickly cooled to 11 K.

Density functional calculations were performed using the Gaussian 98 program.[19] The three parameter hybrid functional, according to Becke with additional correlation corrections due to Lee, Yang, and Parr, was used (B3LYP).[20,21] Recent calculations have shown that this hybrid functional can provide accurate results for the geometries and the vibrational frequencies for transition metal containing compounds.[22,23] The 6-311+G-(d) basis sets were used for N, Cl, and Br atoms, and the all electron basis sets of Wachters−Hay as modified by Gaussian were used for Ni and Cu atoms.[24,25] The geometries were fully optimized and vibrational frequencies were calculated with analytic second derivatives.

Results and Discussion

The FTIR spectra for CuX_2 + N_2 (X = Cl and Br) and $NiCl_2$ + N_2 systems in Ar matrix will be presented in turn with corresponding DFT calculations.

The experiments were done using the $CuCl_2$ and $CuBr_2$ targets with 0.5% N_2 in argon. The spectra in the N−N stretching vibrational region are shown in Figure 1 and the absorptions are listed in Table 1. As shown in Figure 1(a) and 1(b), 1-h co-deposition of the species generated from laser ablated $CuCl_2$ with 0.5% N_2 in Ar resulted in a new absorption at 2296.3 cm^{-1},

* To whom correspondence should be addressed. E-mail: mfzhou@srcap.stc.sh.cn. Fax: 86-21-65102777.

10.1021/jp001171t CCC: $19.00
Published on Web 08/30/2000

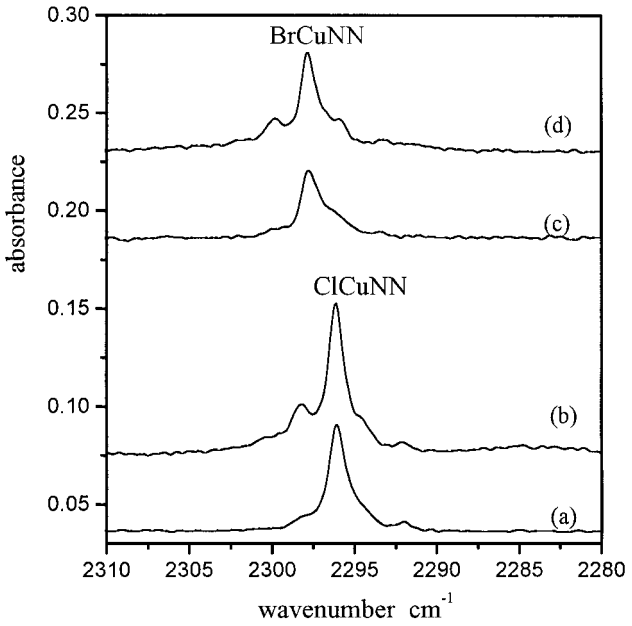

Figure 1. Infrared spectra in the 2310−2280 cm^{-1} region from co-deposition of laser ablated copper halides and N_2 in excess argon. (a) $CuCl_2 + N_2$ (0.5%), 1 h sample deposition at 11 K, (b) after 20 K annealing, (c) $CuBr_2 + N_2$ (0.5%), 1 h sample deposition at 11 K, (d) after 20 K annealing.

TABLE 1: The Observed IR Absorptions (cm^{-1}) of the Products Generated from Co-deposition of Laser Ablated CuX_2 (X = Cl, Br) and $NiCl_2$ Targets with N_2 Molecules in Excess Argon at 11 K.

$^{14}N_2$	$^{15}N_2$	$^{14}N_2 + {}^{14}N^{15}N + {}^{15}N_2$	assignment
2296.3	2219.6	2296.3, 2259.0, 2257.7, 2219.6	ClCuNN
2297.8	2221.0	2297.8, 2260.4, 2259.3, 2221.0	BrCuNN
2246.1	2171.5	2246.1, 2209.6, 2208.5, 2171.5	ClNiNN
2089.4	2019.7	2089.4, 2057.0, 2053.1, 2019.7	NiNN
2103.9	2034.5		$Ni(NN)_2$
2136.3	2064.9		$Ni(NN)_3$
2175.1	2101.5		$Ni(NN)_4$

which increased, apparently on annealing, to 20 K. Besides this, the strong antisymmetric stretching vibrations of the six $CuCl_2$ isotopomers at 513.4, 510.2, 509.3, 506.8, 506.0, and 502.6 cm^{-1} and the four CuCl isotopomers at 420.6, 418.2, 413.9, and 411.6 cm^{-1} were also detected,[26] which were not listed in Table 1. The experiments with a $CuBr_2$ target results in similar absorption at 2297.8 cm^{-1} as shown in Figure 1(c) and 1(d). The $CuBr_2$ and CuBr absorptions are lower than 400 cm^{-1} and were not observed.

Isotopic substitution experiments were done for band identification, and the spectra are shown in Figure 2. In the $^{15}N_2$/Ar experiments, the 2296.3 and 2297.8 cm^{-1} bands were shifted to 2219.6 and 2221.0 cm^{-1}, respectively. In the mixed $^{14}N_2 + {}^{14}N^{15}N + {}^{15}N_2$ experiments, quartets at 2296.3, 2259.0, 2257.7, and 2219.6 cm^{-1} and 2297.8, 2260.4, 2259.3, and 2221.0 cm^{-1} were presented.

A complementary experiment was done with a CuCl target and 0.5% N_2 in argon. The CuCl and the 2296.3 cm^{-1} absorptions were observed as before, but the $CuCl_2$ absorptions were about one-tenth the intensity of the experiments with $CuCl_2$ target. An experiment was also done with $CuCl_2$ target and pure argon gas. The $CuCl_2$ and CuCl absorptions were observed as before, but no distinctive absorption was observed in the N−N stretching region.

Similar experiments were done with a $NiCl_2$ target. Figure 3 presents the infrared spectra in the N−N stretching vibrational

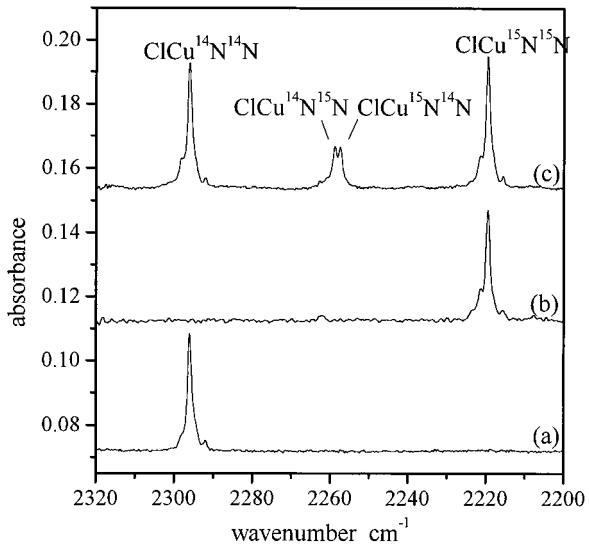

Figure 2. Infrared spectra in the 2320−2200 cm^{-1} region from co-deposition of laser ablated $CuCl_2$ and N_2 in excess argon. (a) 0.5% $^{14}N_2$, (b) 0.5% $^{15}N_2$, (c) $^{14}N_2 + {}^{14}N^{15}N + {}^{15}N_2$ (0.45% + 0.1% + 0.45%).

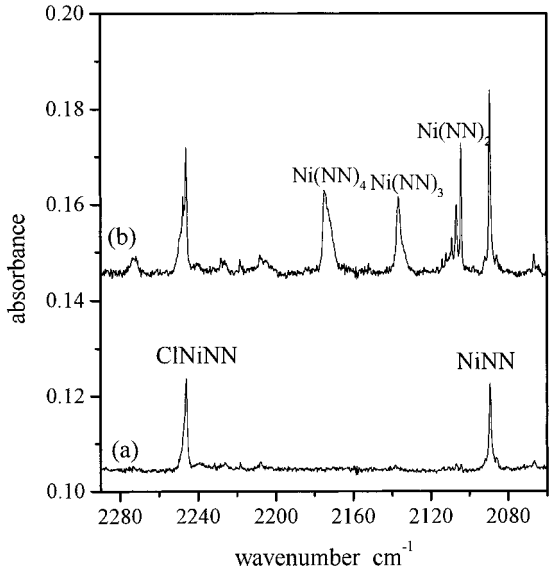

Figure 3. Infrared spectra in the 2300−2050 cm^{-1} region from co-deposition of laser ablated $NiCl_2$ and 0.5% N_2 in excess argon. (a) 1 h sample deposition at 11 K, (b) after annealing to 25 K.

region obtained by co-deposition of laser ablated $NiCl_2$ with 0.5% N_2 in argon at 11 K, and measured before and after annealing. The observed absorption bands are listed in Table 1. Strong $^{58}Ni^{35}Cl_2$ absorption were observed at 520.9 cm^{-1}, but the $^{58}Ni^{35}Cl$ absorption at 418.8 cm^{-1} was hardly detected.[27] In the N−N stretching vibrational region, absorptions at 2246.3 and 2089.4 cm^{-1} were observed after sample deposition and increased upon 25 K annealing. New bands at 2103.9, 2136.3, and 2175.1 cm^{-1} were apparent upon 25 K annealing. Experiments were also done with 0.2% and 1.0% N_2 in argon, and the 2246.3 and 2089.4 cm^{-1} bands were also observed after sample deposition. In the 1.0% N_2 experiment, the 2103.9 cm^{-1} band appeared upon 20 K annealing, the 2136.3 and 2175.1 cm^{-1} bands appeared upon 25 K annealing, and the 2175.1 cm^{-1} band becomes the dominate absorption after 30 K annealing. In the 0.2% N_2 experiment, the 2103.9, 2136.3, and 2175.1 cm^{-1} bands were only observed upon 30 K annealing. The 2246.3, 2175.1, 2136.3, 2103.9, and 2089.4 cm^{-1} shifted to 2171.5,

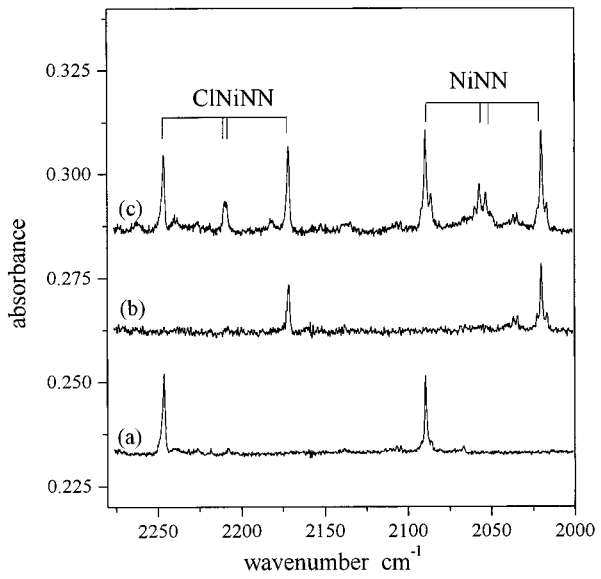

Figure 4. Infrared spectra in the 2275−2000 cm^{-1} region from co-deposition of laser ablated $NiCl_2$ and N_2 in excess argon. (a) 0.5% $^{14}N_2$, (b) 0.5% $^{15}N_2$, (c) $^{14}N_2 + {}^{14}N^{15}N + {}^{15}N_2$ (0.45% + 0.1% + 0.45%).

TABLE 2: Calculated Geometries (Å) and Dissociation Energies (kcal/mol), of the XMN_2, M^+N_2 and MN_2 (X = Cl, Br and M = Cu, Ni) Molecules in Different Coordination Modes[a]

species	R(X−M)	R(M−N)	R(N−N)	De
ClCuNN ($^1\Sigma^+$)	2.091	1.856	1.100	20.4
ClCu(η^2-N_2) ($^1A_1$)	2.096	2.113	1.112	6.7
BrCuNN ($^1\Sigma^+$)	2.218	1.868	1.100	18.7
BrCu(η^2-N_2) ($^1A_1$)	2.221	2.136	1.111	5.6
ClNiNN ($^2\Pi$)	2.090	1.900	1.102	18.9
ClNi(η^2-N_2) ($^2A_1$)	2.112	2.097	1.115	7.4
Cu^+NN ($^1\Sigma^+$)		1.945	1.096	22.2
Cu^+(η^2-N_2) ($^1A_1$)		2.272	1.104	7.8
Ni^+NN ($^2\Sigma^+$)		1.923	1.097	26.2
Ni^+(η^2-N_2) ($^2A_1$)		2.260	1.104	8.2
NiNN ($^1\Sigma^+$)		1.707	1.117	51.5

[a]The energies are corrected with zero point energy.

2102.0, 2064.9, 2033.8, and 2019.7 cm^{-1}, respectively, in the $^{15}N_2$/Ar experiment. In the mixed $^{14}N_2 + {}^{14}N^{15}N + {}^{15}N_2$ experiment, Figure 4, quartets at 2246.3, 2209.6, 2208.5, 2171.5, 2089.4, 2057.0, 2053.1, and 2019.7 cm^{-1} were observed for the 2246.3 and 2089.4 cm^{-1} bands, but the mixed isotopic components for the 2175.1, 2136.3, and 2103.9 cm^{-1} bands could not be resolved due to isotopic dilution.

Calculation Results. At the B3LYP/6-311+G(d) level, the free N_2 bond length was estimated to be 1.096 Å, very close to the experimental value of 1.098 Å. The N−N stretching vibration was calculated at 2444.8 cm^{-1}, which requires a 0.965 scaling factor to fit the experimental value obtained in the gas phase (2359.6 cm^{-1}).[28] DFT calculations were done on XMN_2, M^+N_2, and MN_2 (X = Cl and Br, M = Cu and Ni) molecules with linear end-bonded symmetry and side-bonded C_{2v} symmetry, respectively. The calculated structural parameters and binding energies with respect to XM (or M^+, M) and N_2 are listed in Table 2, and the calculated vibrational frequencies are listed in Tables 3 and 4. For each species, the linear end-bonded structure is more stable in energy than the side-bonded C_{2v} structure. Calculations were also performed on Cl_2CuNN, Br_2-CuNN, and Cl_2NiNN, all three species were predicted to be unbound with respect to $CuCl_2 + N_2$, $CuBr_2 + N_2$, and $NiCl_2 + N_2$, respectively.

ClCuNN and BrCuNN. The 2296.3 cm^{-1} band in the $CuCl_2 + N_2$/Ar reaction was observed on sample deposition and increased on annealing. This band is usually strong when CuCl absorption is strong, and the band intensity increases when increasing the N_2 concentration. It shifted to 2219.6 cm^{-1} with $^{15}N_2$ sample. The isotopic $^{14}N/^{15}N$ ratio 1.0346 indicates that this band is due to a N−N stretching vibration. The isotopic quartet feature in the mixed $^{14}N_2 + {}^{14}N^{15}N + {}^{15}N_2$ experiment suggests that two slightly inequivalent N atoms are involved in this vibration mode. With a $CuBr_2$ target, a 2297.8 cm^{-1} band was observed, which also exhibits N−N stretching vibrational ratio (1.0346) and quartet isotopic structure in the mixed $^{14}N_2 + {}^{14}N^{15}N + {}^{15}N_2$ experiment. The 1.5 cm^{-1} difference between using $CuCl_2$ and $CuBr_2$ targets suggests that the N−N stretching vibrational mode is slightly shifted by the Cl or Br atom. Accordingly, the 2296.3 and 2297.8 cm^{-1} bands are due to the N−N stretching vibrations of the Cl_xCuNN and Br_xCuNN molecules (with $x = 1$ or 2), respectively. The 2296.3 cm^{-1} band was also observed when a CuCl target was used, suggesting that only one Cl atom is most probably involved.

The assignments were further supported by DFT calculations. As has been mentioned, present DFT calculations predicted that the Cl_2CuNN and Br_2CuNN are unbound with respect to $CuCl_2 + N_2$ and $CuBr_2 + N_2$. But DFT calculations predicted that the linear end-bonded ClCuNN and BrCuNN molecules are 13.7 and 13.1 kcal/mol lower in energy than the side-bonded ClCu(η^2−N_2) and BrCu(η^2−N_2) molecules, respectively, and are stable with respect to CuCl + N_2 and CuBr + N_2. The N−N stretching vibrational frequency of ClCuNN and BrCuNN molecules were predicted to be 2383.9 and 2383.2 cm^{-1}, respectively, which both require a 0.96 scaling factor to fit the observed values. The calculated isotopic shifts are also in good agreement with the observed values. As listed in Table 5, the N−N stretching vibration of the $ClCu^{14}N^{15}N$ and $ClCu^{15}N^{14}N$ was predicted to have 1.1 cm^{-1} difference, and the observed difference was found to be 1.3 cm^{-1}. For BrCuNN, the difference between $BrCu^{14}N^{15}N$ and $BrCu^{15}N^{14}N$ was predicted to be 0.9 cm^{-1}, and we observed a 1.1 cm^{-1} separation. The observation of inequivalent nitrogens rules out the side-on structure as the carrier of the observed N_2 vibrations.

No evidence was found for multiple dinitrogen coordination complex on annealing. DFT calculations failed to find stable $ClCu(N_2)_2$ with respect to $ClCu(N_2) + N_2$.

Ni(NN)$_x$ (x = 1−4) The 2089.4 cm^{-1} band observed on sample deposition in $NiCl_2 + N_2$/Ar experiments, and the 2103.9, 2136.3, and 2175.1 cm^{-1} bands appeared on annealing. All of these four bands have been observed in the reactions of thermal or laser ablated Ni atoms and N_2 in argon and are assigned to the N−N stretching vibrations of NiNN, $Ni(NN)_2$, $Ni(NN)_3$, and $Ni(NN)_4$ molecules.[2,5] Our results are in agreement with the previous reports.

ClNiNN. The 2246.3 cm^{-1} absorption was observed after sample deposition when a $NiCl_2$ target was used. This band increased on annealing, and shifted to 2171.5 cm^{-1} in the $^{15}N_2$ experiment. The isotopic 14/15 ratio 1.0344 characterizes this band as a N−N stretching vibration. In the mixed $^{14}N_2 + {}^{14}N^{15}N + {}^{15}N_2$ experiment, a quartet at 2246.3, 2209.6, 2208.5, and 2171.5 cm^{-1} was observed, indicating that two slightly inequivalent N atoms are involved in this molecule. Similar to ClCuNN and BrCuNN, this band is assigned to the N−N stretching vibration of the ClNiNN molecule. The assignment is further confirmed by DFT calculations. As listed in Table 2, the linear ClNiNN is 11.5 kcal/mol lower in energy than the ClNi(η^2-N_2). The N−N stretching vibration was calculated at

TABLE 3: Calculated Vibrational Frequencies (cm^{-1}) and Intensities (km/mol) of $XCuN_2$, and Cu^+N_2 (X = Cl, Br).

ClCuNN	ClCu(η^2-N_2)	BrCuNN	BrCu(η^2-N_2)	Cu^+NN	$Cu^+(\eta^2-N_2)$
2383.9(159) σ	2274.1(115) a_1	2383.2(182) σ	2282.6(125) a_1	2444.4(3) σ	2363.8 (0.2) a_1
454.0(7) σ	417.5(17) a_1	396.9(0) σ	326.7(5) a_1	312.8(0.3) σ	175.9 (3) a_1
313.3(28) σ	215.2(13) a_1	278.6(0 × 2) π	184.3(11) a_1	219.1(2 × 2) π	209.1i (0.2) b_2
290.9(0 × 2) π	100.5(0) b_2	250.5(21) σ	77.9(1) b_1		
73.3(4 × 2) π	93.9(3) b_1	63.9(2 × 2) π	69.4(0.2) b_2		
	75.4(4) b_2		61.6(2) b_2		

TABLE 4: Calculated Vibrational Frequencies (cm^{-1}) and Intensities (km/mol) of $ClNiN_2$ and Ni^+N_2.

ClNiNN	ClNi(η^2-N_2)	Ni^+NN	$Ni^+(\eta^2-N_2)$	NiNN
2357.7(241) σ	2249.3(157) a_1	2431.5(0.1) σ	2358.3(0.1) a_1	2248.1(511) σ
457.6(13) σ	429.9(20) a_1	337.7(0) σ	183.5(2) a_1	543.9(17) σ
311.6(0) σ	235.8(19) a_1	240.1(2 × 2) π	196.7i (0.2) b_2	287.0(6 × 2) π
296.9(19 × 2) π	113.1(3) b_1			
80.2(2 × 2) π	86.5(1) b_2			
	52.2i (10) b_2			

TABLE 5: Comparison of the Observed and Calculated N−N Stretching Vibrational Frequencies of XMNN (X = Cl, Br, M = Cu, Ni) Molecules [a].

	ClCuNN		BrCuNN		ClNiNN	
	obs	cal	obs	cal	obs	cal
$^{14}N_2$	2296.3	2383.9	2297.8	2383.2	2246.3	2357.7
$^{14}N^{15}N$	2259.0(−37.3)	2344.6(−39.3)	2260.4(−37.4)	2343.7(−39.5)	2209.6(−36.7)	2318.5(−39.2)
$^{15}N^{14}N$	2257.7(−38.6)	2343.5(−40.4)	2259.3(−38.5)	2342.8(−40.4)	2208.5(−37.8)	2318.0(−39.7)
$^{15}N_2$	2219.6(−76.7)	2303.4(−80.5)	2221.0(−76.8)	2302.6(−80.6)	2171.5(−74.8)	2278.0(−79.7)

[a] The isotopic shifts relative to the values of $XM^{14}N_2$ are listed in parentheses.

2357.7 cm^{-1}, which must be scaled by 0.95 to fit the observed value. Calculations on Cl_2NiNN converged to $NiCl_2 + N_2$, indicating that the Cl_2NiNN is unbound with respect to $NiCl_2 + N_2$, and rules out the Cl_2NiNN assignment.

For linear XMNN molecules, there are seven vibrational modes. The Cu−Cl and Ni−Cl stretching vibrations of ClCuNN and ClNiNN molecules were calculated to be 65.6 and 64.0 cm^{-1} higher than that of CuCl and NiCl, respectively. As listed in Tables 3 and 4, the NNM−Cl stretching vibrations were predicted to be only about 5% intensity of the N−NMCl stretching vibrations and were too weak to be observed. The other five modes were predicted in the lower frequency region (<400 cm^{-1}), and were not observed in our experiments.

The present characterized ClCuNN, BrCuNN, and ClNiNN molecules are simple dinitrogen complexes and could serve as model compounds for this class of complexes. Weakly bound complexes composed of transition metal cations and closed-shell molecules such as N_2 and H_2 have been studied intensively in recent years.[10,12−17] Quantum chemical investigations found that the ground-state geometries of M^+N_2 species correspond to linear end-on symmetry. Although Asher et al. suggested that $Co^+(N_2)$ possessed a side-bound ground-state, based on the resonant photodissociation spectrum of $Co^+(N_2)$,[9] a combined experimental and theoretical investigation reported by Heinemann et al. showed that the ground state of $Co^+(N_2)$ is indeed linear, and a side-bonded geometry can be excluded.[10] Our calculations show that the Cu^+NN and Ni^+NN are more stable than the side-bonded complexes. In the neutral transition metal-dinitrogen complexes, metal to N_2 electron donation will become a crucial factor in the ground-state geometry due to the absence of a charge on metal center. There is no report on neutral CuN_2 complex, our DFT calculations indicated that CuN_2 is unbound with respect to $Cu+N_2$. Both side-on and end-on bonded neutral NiN_2 complexes have been reported in recent matrix isolation FTIR study of laser-ablated Ni atom reactions with N_2.[5] The NiNN is also observed in our experiments, but no side-bonded Ni(N_2). The NiNN was calculated to have a $^1\Sigma^+$ ground state with σ bonding between Ni and N_2, which results in a shorter Ni−N bond length (1.707 Å) than that of Ni^+NN (1.923 Å) and ClNiNN (1.900 Å). On the basis of our infrared spectra and theoretical calculation results reported here, it is clearly shown that the XMN_2 complexes exhibit end-bonded coordination. However, a complex of CuCl and H_2 produced in argon matrix by co-condensation of CuCl and H_2 was interpreted in terms of a side-bonded ClCu(η^2-H_2).[29] The Difference of coordination modes of ClCuNN and ClCu(η^2-H_2), most probably be due to the different directional properties of the permanent quadrupole moment of H_2 and N_2.[13]

Compared to the free N_2 stretching vibration, the N−N stretching vibrational frequencies of ClCuNN, BrCuNN, and ClNiNN molecules are red-shifted by 63.3, 61.8, and 113.5 cm^{-1}, respectively. This result suggests that the back-donation from metal to N_2 π^* is small. Dinitrogen is generally considered both as a weak σ donor and π acceptor. There are about 0.13 M 3d electron to N_2 π^* donation at the B3LYP level and even less M 3d electron to N_2 π^* donations on the M^+NN cations (about 0.04 electron for Cu^+NN, 0.03 electron for Ni^+NN). The N−N stretching vibrations of Cu^+NN and Ni^+NN were predicted at 2444.4 and 2431.5 cm^{-1}, 60.5 and 73.8 cm^{-1} higher than that of the ClCuNN and ClNiNN molecules. The N−N stretching vibrational frequency of NiNN is red shifted by about 270.2 cm^{-1}, compared to the free N_2, there is about 0.33 electron from Ni to N_2 π^* donation.

The ClCuNN, BrCuNN, and ClNiNN molecules have very similar binding energies. At the B3LYP/6-311+G(d) level of theory, the binding energies of linear XMNN molecules with respect to $MX + N_2$ (M = Cu, Ni and X = Cl, Br) were calculated to be 20.4, 18.7, and 18.9 kcal/mol, respectively, after zero point energy corrections. These values are slightly smaller than the corresponding binding energies of Cu^+NN (22.2 kcal/mol) and Ni^+NN (26.2 kcal/mol) calculated at the same level. Present B3LYP calculations predicted the binding energies quite well. For Ni^+NN, the experimental binding energy with respect to Ni^+ and N_2 has been determined to be 26.5 ± 2.5 kcal/mol,[11] which is in excellent agreement with our calculation value.

Laser ablation of MX_2 targets produces MX_2, MX as the major products. Due to the easy formation of cyclic trimers, it was difficult to obtain CuCl in matrix via thermal evaporation.[29] However, it is easy to produce and isolate the CuCl in argon using laser ablation. When a $CuCl_2$ target was used, the $^{63}Cu^{35}Cl_2$ absorption is about three times stronger than the $^{63}Cu^{35}Cl$ absorption; using the calculated oscillator strengths, the CuCl/$CuCl_2$ ratio in matrix is estimated to be about 0.6. In the $NiCl_2$ experiments, the NiCl absorption is hardly seen, so the NiCl/$NiCl_2$ ratio will be much smaller than the CuCl/$CuCl_2$ ratio. The NiNN absorption was also observed on sample deposition, and the $Ni(NN)_x$ ($x = 2-4$) absorptions were produced on annealing, suggesting that metal atoms were also produced by laser ablation. The failure to observe any absorption of $Cu(NN)_x$ molecules are due to their unstabilities. Our present DFT calculations showed that the optimization of CuNN converged to Cu + N_2. The observed XMNN (X = Cl and Br, M = Cu and Ni) molecules might be formed by the following reactions of MX and N_2, which were calculated to be exothermic. The XMNN absorptions markedly increased on annealing, suggests that reactions 1−3 require no activation energy.

$$CuCl + N_2 \rightarrow ClCuNN \quad \Delta E = -20.4 \text{ kcal/mol} \qquad (1)$$

$$CuBr + N_2 \rightarrow BrCuNN \quad \Delta E = -18.7 \text{ kcal/mol} \qquad (2)$$

$$NiCl + N_2 \rightarrow ClNiNN \quad \Delta E = -18.9 \text{ kcal/mol} \qquad (3)$$

Conclusion

Laser-ablated copper and nickel halides reacted with dinitrogen to give the ClCuNN, BrCuNN, and ClNiNN molecules, which have been isolated in solid argon and identified by isotopic substituted infrared spectra and density functional calculations. Both the infrared spectra and the DFT calculations indicate that these molecules are linear with the N_2 end-bonded to the transition metal atoms. The binding energies for ClCuNN, BrCuNN, and ClNiNN were computationally estimated to be 20.4, 18.7, and 18.9 kcal/mol, respectively.

The excellent agreement with frequencies and isotopic frequency shifts from density functional calculations strongly support the frequency assignments and the identification of these transition metal complexes. These simple transition metal complexes could serve as model compounds for this class of complexes.

Acknowledgment. The authors thank Mr. J. Dong for some experimental work. This work is supported by the Chinese NKBRSF.

References and Notes

(1) Burdett, J. K.; Turner, J. J. *Chem. Commun.* **1971**, 885.
(2) Klatzbucher, W., Ozin, G. A. *J. Am. Chem. Soc.* **1975**, *9*, 7, 2672.
(3) Ozin, G. A.; Vander Voet, A. *Can. J. Chem.* **1973**, *51*, 637.
(4) Chertihin, G. V.; Andrews, L.; Neurock, M. *J. Phys. Chem.* **1996**, *100*, 14 609.
(5) Andrews, L.; Citra, A.; Chertihin, G. V.; Bare, W. D.; Neurock, M. *J. Phys. Chem. A*, **1998**, *102*, 2561.
(6) Beyer, M.; Berg, C.; Albert, G.; Achatz, U.; Joos, S.; Niedner-Schatteburg, G.; Bondybey, V. E., *J. Am. Chem. Soc.* **1997**, *119*, 1466.
(7) Lessen, D. E.; Asher, R. L.; Brucat, P. J. *Chem. Phys. Lett*. **1991**, *177*, 380.
(8) Schwarz, J.; Heinemann, C.; Schwarz, H., *J. Phys. Chem.* **1995**, *99*, 11 405.
(9) Asher, R. L.; Bellert, D.; Buthelezi, T.; Brucat, P. J. *J. Phys. Chem.* **1995**, *99*, 1068.
(10) Heinemann, C.; Schwarz, J.; Schwarz, H., *J. Phys. Chem.* **1996**, *100*, 6088.
(11) Khan, F. A.; Steele, D. L.; Armentrout, P. B., *J. Phys. Chem.* **1995**, *99*, 7819.
(12) Bauschlicher, C. W., Jr.; Pettersson, L. G. M.; Siegbahn, P. E. M., *J. Chem. Phys.* **1987**, *87*, 2129.
(13) Bauschlicher, C. W., Jr.; Partridge, H.; Langhoff, S. R., *J. Phys. Chem.* **1992**, *96*, 2475.
(14) McKee, M. L.; Worley, S. D., *J. Phys. Chem. A*, **1997**, *101*, 5600.
(15) Ogden, J. S.; Sweany, R. L.; Rest, A. J. *J. Phys. Chem.* **1995**, *99*, 8485.
(16) Ogden, J. S.; Sweany, R. L. *Inorg. Chem*. **1997**, *36*, 2423.
(17) McKee, M. L.; Sweany, R. L. *J. Phys. Chem. A*, **2000**, *104*, 962.
(18) Chen, M. H., Wang, X. F., Zhang, L. N., Yu, M., Qin, Q. Z. *Chem. Phys.* **1999**, *242*, 81.
(19) Frisch, M. J.; Trucks, G. W.; Schlegel, H. B.; Scuseria, G. E.; Robb, M. A.; Cheeseman, J. R.; Zakrzewski, V. G.; Montgomery, J. A., Jr.; Stratmann, R. E.; Burant, J. C.; Dapprich, S.; Millam, J. M.; Daniels, A. D.; Kudin, K. N.; Strain, M. C.; Farkas, O.; Tomasi, J.; Barone, V.; Cossi, M.; Cammi, R.; Mennucci, B.; Pomelli, C.; Adamo, C.; Clifford, S.; Ochterski, J.; Petersson, G. A.; Ayala, P. Y.; Cui, Q.; Morokuma, K.; Malick, D. K.; Rabuck, A. D.; Raghavachari, K.; Foresman, J. B.; Cioslowski, J.; Ortiz, J. V.; Baboul, A. G.; Stefanov, B. B.; Liu, G.; Liashenko, A.; Piskorz, P.; Komaromi, I.; Gomperts, R.; Martin, R. L.; Fox, D. J.; Keith, T.; Al-Laham, M. A.; Peng, C. Y.; Nanayakkara, A.; Gonzalez, C.; Challacombe, M.; Gill, P. M. W.; Johnson, B.; Chen, W.; Wong, M. W.; Andres, J. L.; Gonzalez, C.; Head-Gordon, M.; Replogle, E. S.; Pople, J. A. *Gaussian 98*, Revision A.7, Gaussian, Inc.: Pittsburgh, PA, **1998**.
(20) Becke, A. D., *J. Chem. Phys.* **1993**, *98*, 5648.
(21) Lee, C., Yang, E., Parr, R. G., *Phys. Rev. B*, **1988**, *37*, 785.
(22) Bauschlicher, C. W. Jr., Ricca, A., Partridge, H., Langhoff, S. R. In *Recent Advances in Density Functional Theory*; Chong, D. P., Ed.; World Scientific Publishing: Singapore, **1997**, Part II.
(23) Bytheway, I., Wong, M. W. *Chem. Phys. Lett.* **1998**, *282*, 219.
(24) McLean, A. D., Chandler, G. S. *J. Chem. Phys.* **1980**, *72*, 5639. Krishnan, R., Binkley, J. S.; Seeger, R.; Pople, J. A. *J. Chem. Phys.* **1980**, *72*, 650.
(25) Wachter, J. H. *J. Chem. Phys.* **1970**, *52*, 1033. Hay, P. J. *J. Chem. Phys.* **1977**, *66*, 4377.
(26) Martin, T. P.; Schaber, H. *J. Chem. Phys.* **1980**, *73*, 3541.
(27) Nakamoto, K. *Infrared and Raman Spectra of Inorganic and Coordination Compounds*, 1977.
(28) Huber, K. P.; Herzberg, G. *Molecular Spectra and Molecular Structure IV. Constants of Diatomic Molecules*; Van Nostrand: Toronto, 1979.
(29) Plitt, H. S.; Bar, M. R.; Ahlrichs, R.; Schnockel, H. *Angew. Chem., Int. Ed. Engl.* **1991**, *30*, 832.